



HAL
open science

MWCNTs/PMMA/PS composites functionalized PANI: electrical characterization and sensing performance for ammonia detection in a humid environment

Sahal Saad Ali

► To cite this version:

Sahal Saad Ali. MWCNTs/PMMA/PS composites functionalized PANI: electrical characterization and sensing performance for ammonia detection in a humid environment. *Sensors and Actuators B: Chemical*, 2020, 320, pp.128364. 10.1016/j.snb.2020.128364 . hal-02954409

HAL Id: hal-02954409

<https://hal.inrae.fr/hal-02954409>

Submitted on 22 Aug 2022

HAL is a multi-disciplinary open access archive for the deposit and dissemination of scientific research documents, whether they are published or not. The documents may come from teaching and research institutions in France or abroad, or from public or private research centers.

L'archive ouverte pluridisciplinaire **HAL**, est destinée au dépôt et à la diffusion de documents scientifiques de niveau recherche, publiés ou non, émanant des établissements d'enseignement et de recherche français ou étrangers, des laboratoires publics ou privés.



Distributed under a Creative Commons Attribution - NonCommercial 4.0 International License

MWCNTs/PMMA/PS composites functionalized PANI: electrical characterization and sensing performance for ammonia detection in a humid environment

Sahal SAAD ALI ^{1,2*}, Alain Pauly ¹, Jérôme Brunet ¹, Christelle Varenne ¹, Amadou L. Ndiaye ^{1*}.

(1) Université Clermont Auvergne, CNRS, Sigma Clermont, Institut Pascal, F-63000 Clermont-Ferrand, France,

(2) Institut de Chimie de Clermont-Ferrand (ICCF)-UMR 6296, Université Clermont Auvergne

Phone: 33 (0)4 73 40 72 38 / Fax: 33 (0)4 73 40 73 40

Emails: amadou.ndiaye@uca.fr / sahasad43@gmail.com

ABSTRACT:

This work aims to develop stable and reliable sensor films based on polyaniline (PANI) composites able to detect ammonia in a humid environment. For the preparation, PANI is hosted in poly(methyl methacrylate) (PMMA)/polystyrene (PS) blends matrix and to optimize the electrical properties, multi-walled carbon nanotubes (MWCNTs) are added into the matrix. The preparation method alternating heating and ultrasonic treatment leads to good dispersion and ensure stable films. The materials are characterized by infrared (IR) spectroscopy, scanning electron microscopy (SEM) and electrical characterizations. The temperature-dependent electrical measurement showed that PANI governed the electrical properties in the composites. The resistive sensors based on such composites are tested for ammonia detection and the composite based especially on PANI/PMMA/PS/MWCNTs shows the best sensor performances, with a linear sensitivity in the 5-20 ppm range, a limit of detection (LOD) averaging 830 ppb and response and recovery time estimated to 270 and 630 seconds respectively. Furthermore, it presents repeatable responses and very good stability in a humid environment as well as long-term stability. The preparation way is an essential point to reach these performances that result from a synergetic contribution of all elements.

KEYWORDS: Polyaniline, PMMA/PS Blends, Resistive, Sensors, Ammonia, Humidity

1. INTRODUCTION

In front of the increasing amount of sources of pollution, it has become vital to monitor and detect pollutants (toxic gases) to limit their impacts and prevent from the exposition. Among these toxic gases, hydrogen sulfide (H_2S)[1], ammonia (NH_3)[2], carbon monoxide (CO)[3], nitrogen oxides (NO_x)[4], etc. are commonly produced by man-made and industrial processes. Among the gases species classified as species to be monitored NH_3 is of major importance since it can seriously impact our health. For humans, for instance, inhalation of a higher concentration of NH_3 (over 300 ppm) is enough to induce accidents with irreversible effects depending on the concentration and exposition duration. At approximately 15-28% by volume in air, NH_3 is also flammable [5]. For these reasons, threshold limit values (TLV) for NH_3 corresponding to long-term and short-term exposure have been established. These values are 25 ppm during 8 h, for long-term exposure and 35 ppm during 15 min for short-term exposure [6]. But another worrying effect is that ammonia can be also produced during the fermentation process in bioreactors [7]. Taking into account that, as a source of renewable energy, biogas or bioenergy production is becoming more and more significant, it might be also envisaged to monitored such biogas production plants to protect both workers and digesters. In fact, ammonia can not only seriously affect the efficiency of biogas production [8] but can be also dangerous for workers in such bioreactors. The development of sensors for monitoring such environment required that also the sensors film resist to an environment with a high level of humidity, a condition that is not satisfied by PANI alone.

To monitor these pollutants, the chemical sensors have attracted great interest in the detection of various toxic gases. In the last decades, materials for chemical sensors are mainly covered by three categories of materials having all advantages and drawbacks: metal oxide (MOX), carbon materials (CNTs and graphene), conducting polymers (CPs) and any combination of these materials [9-10]. For MOX, higher temperature operating conditions and the lack of selectivity are the common drawbacks. In recent years, a combination of MOX with other matrices such as CNTs or CPs has been developed and in some combinations (MOX with CPs and /or CNTs) for example, the operating temperature of the hybrid sensing structure can be drastically lowered compared to parent MOX structure [11-13]. Carbon nanotubes have attracted great

interest in recent years in the field of sensors because of their unique structure and the high surface-to-volume ratio [9, 14-16] combined to their ability to detect both oxidizing and reducing gases and also a wide range of organic vapours [17-21]. CNT-based sensors have some limitations such as moisture sensitivity and lack of selectivity to analytes for which they have low adsorption energy or low affinity. In order to overcome and improve the sensitivity and selectivity of CNTs, lots of effort are being focused on functionalization. However, as materials with good electrical properties, CNTs can be used also as a filler in polymer matrices to improve the electrical properties of the polymer matrix [9, 22-23].

Frequently used conjugated polymers for the development of gas sensors are PANI, polypyrrole (PPy) and polythiophene (PT). Among conducting polymer there is an increasing number of studies associating polyaniline as sensing materials [24] for NH_3 . PANI has been investigated as a potential sensing material due to its controllable electrical conductivity, good sensitivity at room temperature and relative ease of processing [25]. Polyaniline presents different electronic properties inherent to its oxidations states which make it suitable for sensing applications [26-29]. However, PANI suffers from the lack of solubility and infusibility leading to mechanical instability [30]. In fact whatever the synthesis way (powder, fibers, solid), PANI adhere not easily to surface devices. This is a common problem encountered in conjugated polymers and is mainly attributed to high polarizability and high backbone rigidity [24]. Others difficulties concerns the fact that PANI reacts with gaseous species in acid-base reaction [31] which can lead to swelling of the structure [32]. Therefore PANI has been also combined with polymers such as PMMA [31, 33-34] or PS [35] blends or carbonaceous matrix [20, 36] to improve mechanical stability.

PANI functionalized MWCNT have been found to be sensitive for ammonia detection, however, poor recovery of the sensor was noticed in many of these reports [29, 31, 37]. Having an objective to reinforce the PANI structure and its mechanical stability we have focused on the use of PMMA/PS blend which has proven to be an adequate mixture to reinforce the tensile strength and the mechanical and conducting properties [38]. The presence of the PS (hydrophobic)[39-40] also can be a judicious point for tuning the reactivity in humid environments. To this polymer blend, we have also added CNTs to improve the conductivity of the blend while conserving the main sensing properties from the PANI. To realize such structures (multi-components polymer blends), many

strategies to associate polymers with nanocharges (CNTs and/or PANI), starting from simple methods to more elaborated ones, have been established. The simple methods of preparation consist in general mixing like solution mixing or melt mixing [41], mechanical mixing [42], while more complex methods can be coating PANI with electrospun PMMA [34, 43], scanned-tip electrospinning method [44], simple electrospinning [69], spin coating [40]. However, apart from the preparation methods, the stability of the polymer matrix blends is also important if at least more components are involved in the polymers matrix. A combination of the individual polymer component, to build a complex polymer blend has been theoretically described and it seems that a good association is mainly dependent on the surface tension of the individual polymers [45]. In other studies [38, 42], it has been shown that using a compatibilizer can facilitate the matching of the different components in the polymer complex and therefore allow us to realize stable films. PANI has been reported to act as a compatibilizer in complex polymer blends due to its high surface tension and polarity [46].

In these methods, fibers-like polymers blends structures, as well as polymeric films can be generated and used as sensors. But, the stability of these sensing materials, made of several components, after routinely gas sensing exposures or experiments in a humid environment is not always guaranteed. Furthermore conjugated polymers blends, in either fibers-like forms or in film forms, often experience moisture/humidity sensitivity [47], [48], [49], [40], [50]. In our case, we will adopt a simple and low-cost method alternating heating and ultrasonic treatment in which sonication and heating under stirring ensure in one side to obtain a good and stable film without using a compatibilizer and on the other side, the perfect matching of the different components to circumvent test under humid environment.

In this paper, we will associate the polymer blend PMMA/PS with CNTs to isolate composite materials which can be used as a stable matrix to host PANI fibers to form our sensing materials (PANI/PMMA/PS/MWCNTs). The electrical characteristics of these materials will be analyzed and the sensing performance towards ammonia will be finely discussed. A special focus will be on the stability and the responses to the ammonia of this composite in a humid environment.

2. EXPERIMENTAL PART

2. 1. Materials and solvents

Acetone, acetonitrile, methanol, and ethanol were purchased from Aldrich and used as solvents. Aniline, methyl methacrylate (MMA), styrene, sulphuric acid (H_2SO_4 (0.5 M)), nitric acid (HNO_3), ammonium peroxydisulfate ($(\text{NH}_4)_2\text{S}_2\text{O}_8$), benzoyl peroxide (BPO) and N,N-Bis(2-hydroxyethyl)-p-toluidine (p-toluidine) are purchased from Aldrich and used as reagents without further purification. MWCNTs were obtained from Helix materials solution.

2. 2. Materials preparation.

Synthesis of MWCNT-OH: The MWCNTs surfaces were prepared using the chemical oxidation for anchoring functional groups for better cohesion between the MWCNTs and the polymer. 150 mg MWCNT are dispersed in acidic media ($\text{H}_2\text{SO}_4/\text{HNO}_3$, volume ratio 3:1). The mixture is then sonicated for 20 minutes and heated at 70 °C during 8 h under stirring. The resulting black mixture is then filtered and washed several times with deionised water. The powdered material is finally washed with ethanol and dry at 100 °C for 5 h.

Synthesis of the non-conducting Polymers (PMMA, PS and PMMA/PS blends):

PMMA: 20 ml of the MMA monomer was mixed with 20 mg of BPO and 160 mg of p-toluidine. This mixture is then heated under stirring to reach 90°C. The polymerisation starts to take place after 20-30 minutes of stirring at 90 °C. Soon after (5-10 minutes) the formed PMMA can be either isolated or used in its viscous form for further reaction.

PS: 10 ml of the styrene monomer was mixed with 10 mg of benzoyl peroxide and 160 mg of p-toluidine. This mixture is then heated under stirring to reach 90 °C. The polymerisation starts to take place after 30 minutes of stirring at 90 °C. At this stage, the obtained PS can be either isolated or used for further reaction.

PMMA/PS blends: In a flask, 0.5 ml of PMMA (65 mg) and 0.5 ml of PS (65 mg) are mixed in acetone and sonicated for 20 minutes at room temperature. The resulting PMMA/PS foamy polymer is then collected and heated at 75 °C the viscous liquid starts to form after 10 minutes of heating under stirring. The resulting mixture can be used in further steps.

Synthesis of the conducting polymer (PANI-H₂SO₄ doped): Polyaniline was prepared using the oxidative polymerization method using ammonium persulfate and sulphuric acid (H₂SO₄) as a dopant. In an example of synthesis 10 mL of aniline was cooled using an ice bath (0 °C) and 25 ml of a diluted solution of H₂SO₄ (0.25 M) was added under stirring to aniline and gives rise to a white salt-like mixture. To this mixture, was drop wisely added in an acidic solution of ammonium peroxydisulfate (31.26 g in 30 ml H₂SO₄). The white dispersion turns brown after the first drop and ends up with a green coloration at the end of the process. The resulting mixture was allowed to stay under stirring for 24 hours. The mixture is then filtered and washed with acidic water (100 ml H₂O + 50 ml H₂SO₄ 0.5 M) before being stored at room temperature. The resulting powdered PANI can be re-dispersed in acetonitrile for the coating process.

Synthesis of PANI/PMMA/PS/MWCNTs composites: In a flask, 1ml of PMMA/PS in acetone is sonicated for 20 minutes at room temperature. The resulting PMMA/PS foamy polymer is then collected and the MWCNTs-OH solution (1 mg MWCNTs-OH dispersed in acetonitrile) corresponding to 0.7% weight (MWCNTs) were injected into the polymer solution under sonication. For electrical optimization the filler (MWCNTs) content in weight percentage into the polymers blend (PMMA/PS) was varied at 3.5% (4.7 mg of MWCNTs), 7% (10 mg of MWCNTs) and 10% (15 mg of MWCNTs). The resulting grey/black mixture is sonicated during 15 minutes and 5 mg of PANI (dispersed in acetonitrile) is carefully injected to the mixture under sonication and further 15 minutes of sonication is performed. This corresponds to approximately 3.3-3.8% weight of PANI in the composites. The resulting mixture is then heated at 90 °C for 10 minutes and results in a viscous green mixture. This later is then sonicated and heated in an alternating way to ensure good dispersion (protocol 1 in Scheme 1). Alternatively, a process consisting of either heating or sonicating (protocol 2 in Scheme 1) the mixture can be applied but this later does not allow to prepare homogeneous materials and stable films for our application.

For comparison, PANI/PMMA/PS and PANI/PS composites (without MWCNTs) were also synthesized using the same procedure to evaluate the MWCNTs' effect. Table S1 (see supporting information file) gathers the composites' contents and preparation conditions.

2. 3. Materials characterization.

Unless otherwise stated all characterizations were conducted at room temperature. Scanning Electron Microscopy (SEM) micrographs are obtained from a JEOL 6060 Low Vacuum operating at 5 kV. The samples were prepared by drop-casting the sensing materials on copper substrates followed by drying at room temperatures. Fourier transform infrared spectrometry (FTIR) spectra are recorded in the attenuated total reflexion (ATR) mode using a Nicolet 5700 FTIR spectrometer in the mid-IR region 4000-400 cm^{-1} and with a resolution of 4 cm^{-1} .

2. 4. Sensors preparation.

For the realization of resistive sensors, interdigitated electrodes (IDEs) made of platinum screen printed on an alumina substrate, with an inter-electrode distance of 125 μm (wide x length = 3mm x 5mm), were used. Both PANI and the polymer composites were thoroughly dispersed in acetonitrile and coated on IDEs. The coated IDEs were allowed to dry at room temperature and used as resistive devices for the sensing experiments. The electrical characteristics (I-V curves) were obtained from Keithley 2636 System Source Meter which is controlled by a Labview program. For the electrical characterization, the voltage was scanned from -1 V to +1 V while recording the current. Temperature dependence measurements of the sensors were carried out by adapting the measurement chamber with a cryostat device (filled with liquid nitrogen) which enables operating temperatures from 170 K up to 500 K.

2. 5. Gas sensing experiments.

For gas exposure experiments, a dilution bench consisting of pollutant sources, the chamber, and a computer-assisted data acquisition and collection program monitored through a Labview software was used to study the gas sensing performances. The gas source (gas cylinders) was diluted with dry air (corresponding to a relative humidity of

around 3-5 %) to obtain the desired concentration range. For relative humidity experiments, a humidity control unit is adapted to the test bench to provide between 10% and 70% of relative humidity. For monitoring the sensors resistance variation under gas exposure a Digital Multimeter (Keithley 2700) was used.

The resistance variation of the sensors under successive gas exposure will be given as a function of the gas concentration. For the resistive sensor's analysis as presented in the calibration curves, the sensors' responses are represented by their $\Delta R/R_0$ values, using the following formula:

$\Delta R/R_0 = (R_{Gas} - R_0)/R_0$ where $\Delta R = R_{Gas} - R_0$; this $\Delta R/R_0$ value can be also expressed in % by multiplying with a factor 100.

In this formula, ΔR is the resistance variation caused by gas exposure and is defined as the difference between resistance under air zero (R_0) and resistance under gas (R_{Gas}). The resistance under air zero is calculated by averaging the ten last values of the resistance under recovery while R_{Gas} is taken the maximum resistance under gas exposure.

Response time (τ_{resp}) is defined as the time needed to reach 90% of the maximum response amplitude while recovery time (τ_{rec}) is defined as the time needed to recover 90% of the background signal.

Sensitivity (S) of the sensors is defined as the sensor's response per unit concentration (ppm) detailed in the following formula:

$$S = \Delta R/R_0 (\%)/\text{Concentration (ppm)}$$

Therefore, for the resistive sensors, the sensitivity is accordingly presented in % /ppm. For the comparison with other articles, responses can be also expressed in percentage at a given concentration corresponding to $\Delta R/R_0$ in % at x ppm as presented in Table 1.

3. RESULT AND DISCUSSION

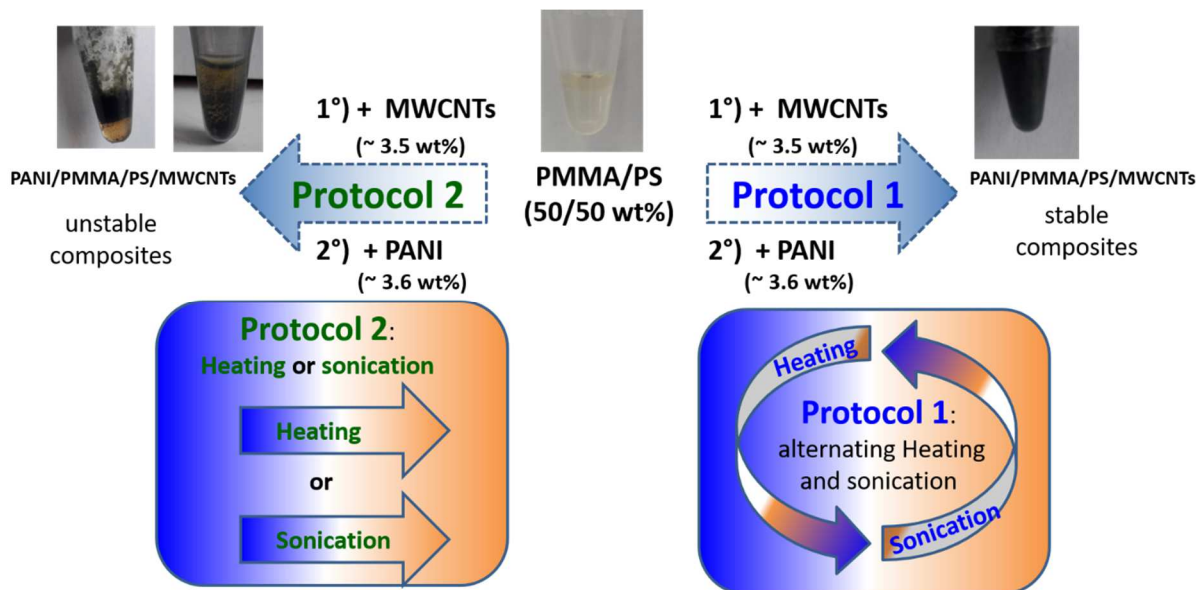
From the previous remarks concerning the lack of solubility and infusibility of PANI [30], we have prepared polymer composites based on PANI, PMMA, PS, and MWCNTs. In this synthesis PANI is the principal element, the supporting matrix PMMA/PS blend is

supposed to serve as a polymer matrix able to rigidify the sensing structure while keeping the conductive properties of PANI. The MWCNTs are added to ensure good conductivity for the PMMA/PS blends by implementing an additional conducting path.

3. 1. Materials synthesis: importance of the preparation protocol.

PANI has been synthesized using the oxidative method. This conductive polymer is known for its easy synthesis way in which a wide variety of acids such as hydrochloric acid [27, 51], sulphuric acid [52], etc. can be used and several morphologies can be obtained [53-54]. In our case, we used sulphuric acid as a dopant and ammonium persulfate as an oxidant to prepare the conductive polymer material and we isolated fiber-like materials as revealed later in the SEM characterization. Afterward PMMA and PS have been synthesized separately and mixed together in a 50%/50% weight ratio forming the PMMA/PS blends. In fact, it has been reported that the PMMA/PS blend in such a ratio allows isolating polymers blends with good tensile strength and electrical properties [38]. As already published, the MWCNTs can bridge the different conducting domains in the matrix [51]. In other configuration, the incorporation of an optimum quantity of CNT in PANI matrix can even increase mechanical stability by preventing the large volumetric change leading to instability of the layers [27]. As we will see, adding MWCNTs and the PANI to the polymer mixture has been proven to improve the electrical properties (see electrical characterization). For the following, we have chosen to work with 3.5 % - 4 % in percentage weight of fillers corresponding to the concentration below the percolation threshold for PANI [30, 38] and MWNTs [22] even if a higher percentage of PANI can be found for PANI/MWCNTs composites [20, 33].

In both the incorporation of PANI or MWCNTs to the PMMA/PS matrix, the amount of fillers is important but more attention has been put on the preparation protocol (scheme1). In fact, both PANI and MWCNTs are not soluble in this polymer matrix (PMMA/PS) which means that they cannot build a homogenous and stable film with the polymer matrix. Trying to disperse them by either heating or sonication (protocol 2) has failed since the mixture was unstable: i) the polymer matrix was separated from the PANI+MWCNTs few times after the end of the reaction if heating was chosen, ii) while the PANI+MWCNTs re-aggregate few seconds after the end of the reaction if sonication was chosen.



Scheme 1: Preparation details showing the specific synthesis protocols leading to the formation of PANI composites.

Therefore we apply a special protocol mixing these two procedures in an alternating way (protocol 1). Therefore, to the polymer mixture (PMMA/PS), we have added MWCNTs (3.5 wt%) and PANI (3.6 wt%) following the protocol 1 alternating heating and ultrasonic treatment to ensure a good dispersion of the filler (PANI or/and MWCNTs) into the matrix as presented in Scheme 1 and later in Fig. 2 (C and D). The PANI+MWCNTs are dispersed and debundled through sonication while heating under stirring speeds up the polymerization and ensures the homogeneity. Alternating these two steps guarantees the stability and homogeneity of the blends as we will see in the SEM and IR characterizations. While the protocol 2 leads to unstable composites (see Scheme 1 and later Fig 2 B), protocol 1 has been evaluated as fitting perfectly to the synthesis of polymer blends associating different components.

To complete this study, other composites without MWCNTs or with higher MWCNTs contents discussed in this article are also prepared using the same protocol. Readers can refer to Table S1 in the supporting information file for more information in the composites' preparation conditions.

3. 2. Characterization by IR spectroscopy.

IR spectrum of the PANI-composite is displayed in Fig. 1 and for comparison, the other non-conducting polymers constituting the composite are also presented. For a better analysis of the structure, we first analyzed the PANI itself (black spectrum in Fig. 1)

which constitutes the major element in the composite. The presence of strong peaks between $1450 - 1530 \text{ cm}^{-1}$ and between $1540 - 1600 \text{ cm}^{-1}$ is attributed to aromatic ring stretching ($\text{C}=\text{C}$) of the benzenoid and quinonoid unit in PANI respectively [53, 55-58]. The fact that the intensity of the quinoid band at 1600 cm^{-1} is weaker compared to the benzenoid band at 1500 cm^{-1} is confirmation that the emeraldine salt form of polyaniline has lower conjugation as result of acid doping. However, as already mentioned in the previous publications, the band characteristic of the conducting protonated form of PANI is observed at 1243 cm^{-1} and is assigned to a stretching vibration in the polaron structure [53, 59]. Other characteristics peaks are also revealed: out-of-plane and in-plane bending vibrations of C-H are found in the region $750 - 850 \text{ cm}^{-1}$ and $1085 - 1200 \text{ cm}^{-1}$ while C=N and C-N stretching vibrations are localized peaks around $1200 \text{ cm}^{-1} - 1380 \text{ cm}^{-1}$ [55]. The peak at 3228 cm^{-1} is attributed to the N-H stretching.

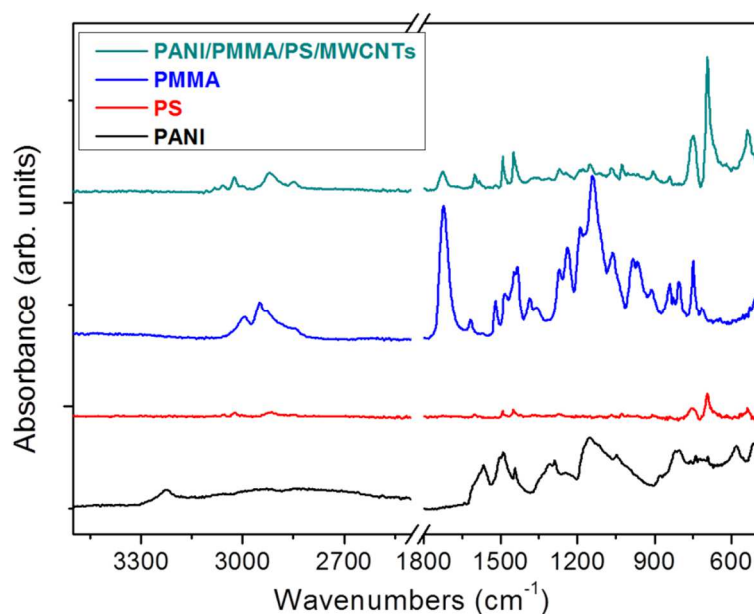


Fig. 1: FTIR spectra of composite PANI/PMMA/PS/MWCNTs (MWCNTs 3.5 wt%), PMMA, PS, and PANI.

The characteristic band at 1722 cm^{-1} in the PANI/PMMA/PS/MWCNTs (3.5 wt%) composite is assigned to the $\text{C}=\text{O}$ stretching modes of vibration of the carbonyl group from the PMMA. The peak at 692 cm^{-1} is attributed to the presence of PS in the matrix while the larger peak at 748 cm^{-1} is a superposition of PMMA and PS (from the PMMA/PS blend). It should be noted here that the MWCNTs are not visible since they are embedded in the matrix. The PANI peaks are falling within the region where the PMMA/PS matrix presents strong peaks, and are therefore not easy to be attributed. In the region $2800 - 3200 \text{ cm}^{-1}$, we can identify peaks ($>3000 \text{ cm}^{-1}$) representing both the

C_{sp^2} -H stretching (PS) and those ($<3000\text{cm}^{-1}$) representing the C_{sp^3} -H stretching (PMMA).

3.3. SEM analysis.

SEM analysis has been performed on polymer composites used in the sensor devices. For comparison, PANI has been also characterized by SEM and presented in Fig. 2a. In this figure, the PANI is organized like small fibers but aggregates of non-fibrous morphology were also present in the samples to some extent. Such a morphology has been already observed for PANI synthesized in acidic media [54, 60]. The fibers have generally diameters averaging 100 nm but they can collapse and reach larger aggregates ($\sim\mu\text{m}$ range). In Fig. 2b SEM micrograph of PANI/PMMA/PS/MWCNTs prepared through protocol 2 is shown and we can distinctly identify the polymer matrix and the PANI/MWCNTs islands sitting on its top evidencing an unstable composite.

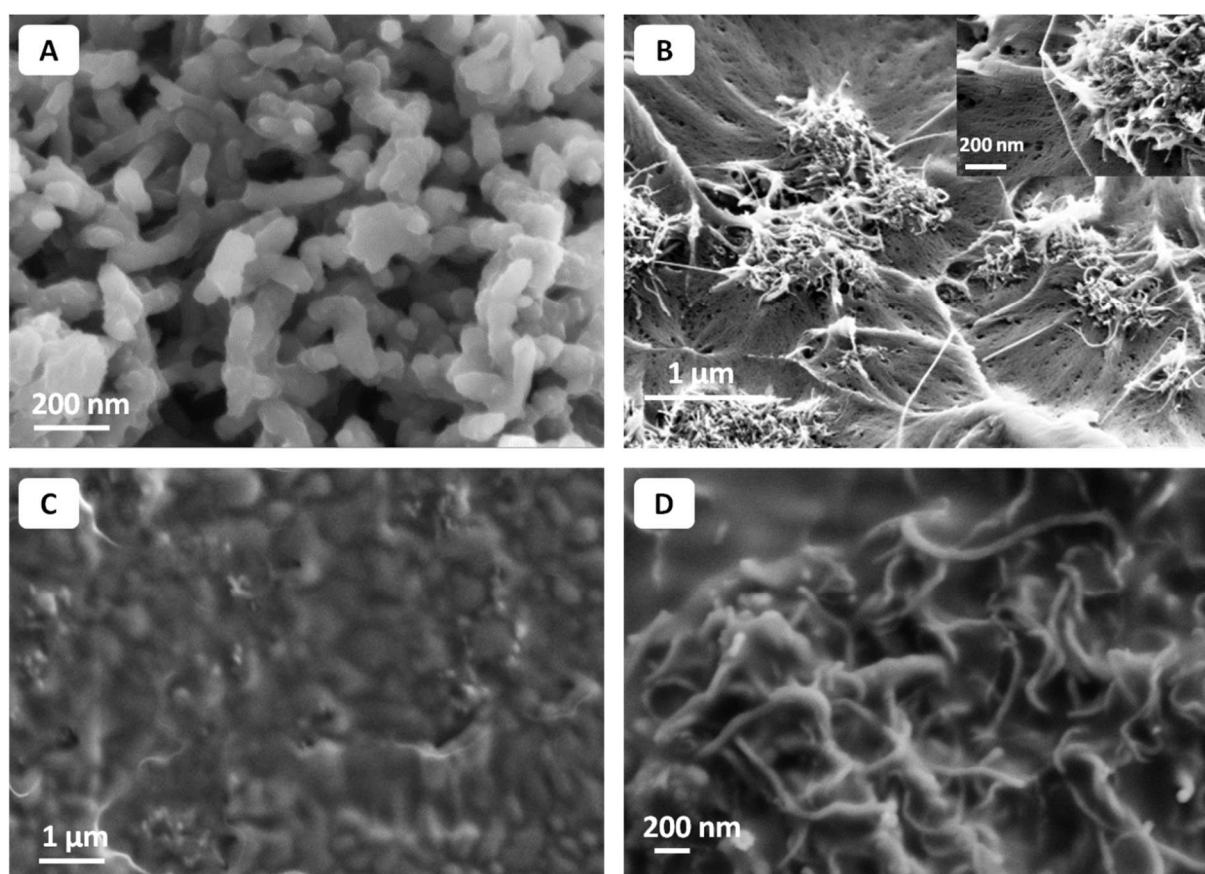


Fig. 2: SEM images of a) pure PANI, b) composite (MWCNTs 3.5 wt%) prepared by protocol 2, c) composite (MWCNTs 3.5 wt%) prepared by protocol 1, and d) a zoom on the composite prepared by protocol 1.

In Fig. 2c the SEM image represents a rather stable film of PANI/PMMA/PS/MWCNTs obtained through the special protocol method alternating

heating and sonication. A zoomed image as presented in Fig. 2d allow identifying embedded fibers and wires representing the PANI and MWCNTs. Unlike the image in Fig. 2B, in Fig. 2c and 2d the surface of the composite appears rough and smooth attesting the adequate. In the composite prepared trough protocol 1, the morphology suggests that all elements are present together with PANI and they synergistically act as a unique surface giving rise to a mechanically stable structure. This morphology resembles that from Rozik et al. [38] who evidenced an increase in interaction (leading to a smooth surface) due to the reduction in domain sizes if PANI is added to the PS/PMMA blend. In their work, Rozik et al. [38] explained this result by the role played by pluronic together with PANI acting as a mechanical compatibilizer between PS and PMMA. We can say here that we came to the same result through applying a protocol which plays the role of compatibilizer between PS and PMMA.

A zoom on such surface (Fig. S1) allows seeing also that the MWCNTs are embedded in the PMMA matrix. Even if the PANI looks like islands separated by PMMA/PS blend on the top of the surfaces, electrical connections are ensured by both PANI and MWCNTs into the volume. This will be further confirmed through electrical characterization.

3. 4. Electrical characterization.

For this study, we have chosen to further experiment the PANI/PMMA/PS/MWCNTs composites in which the MWCNTs are 0.7-10% in weight and this corresponds to a PANI weight percentage averaging 3.6%. Fig. 3 represents characteristic curves at room temperature of the composites by varying the MWCNTs amount in the synthesized materials. PANI composites were layered on IDEs to perform current-voltage characteristics. For the electrical characterization, the current-voltage (I-V) characteristics were acquired within the range of -1 V to $+1$ V.

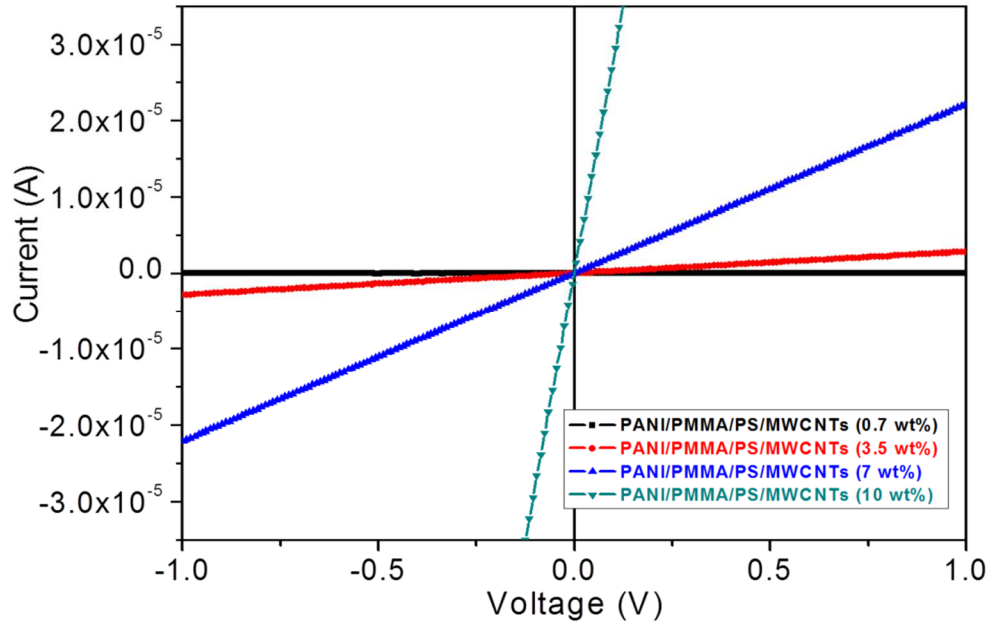


Fig. 3: I-V Electrical characteristics of composite (PANI/PMMA/PS/MWCNTs) with different MWCNTs contents 0.7 wt% (green), 3.5 wt% (black), 7 wt% (blue), and 10 wt% (red) at room temperature ($\sim 28^\circ\text{C}$).

All PANI composites based layers exhibited perfect ohmic behavior. This ohmic behavior clearly indicates that charge carriers are able to flow smoothly between the platinum electrodes through the polymer sensing material network. At higher MWCNTs contains (10%) the resistance was lower but still we conserved an ohmic behavior. But in such a configuration the conductivity was dominated by the MWCNTs part. Up to now and in the following discussion “PANI/PMMA/PS/MWCNTs” denotes the composite in which the MWCNTs are 3.5% in weight and PANI 3.6%. We have chosen to work with such concentration corresponding to the concentration below the percolation threshold for PANI [30, 38] and MWNTs [22]. At such concentrations of PANI and MWCNTs, we are below the percolation threshold and we have correct resistance value that allow us to further investigate the action of NH_3 . Working with higher MWCNTs concentrations will lead to films with lower resistance of course but the response will be dominated by the MWCNTs more than the PANI.

It is well accepted that the conduction mechanism in conducting polymers such as PANI is very complex since these materials exhibit a wide range of conductivity from insulator to metallic leading to different mechanisms within different regimes [61]. To analyze the conduction mechanism, we conducted temperature-dependent current-voltage characteristics of the PANI-based composites by recording the resistance

variation. While most of the studies focus on either higher temperature or lower temperature, for our study, we extend the temperature in both lower and higher temperature regime, i.e. from 180 K to 400 K. Fig. 4 shows the temperature dependence curve of PANI-based composites and for the comparison, we added the corresponding curve for PANI. Both PANI and PANI composites show a non-monotonic resistance variation. In fact, for both materials, the resistance decreases until 325 K for PANI and 380 K for PANI composites and then rises from these temperatures respectively to 460 K.

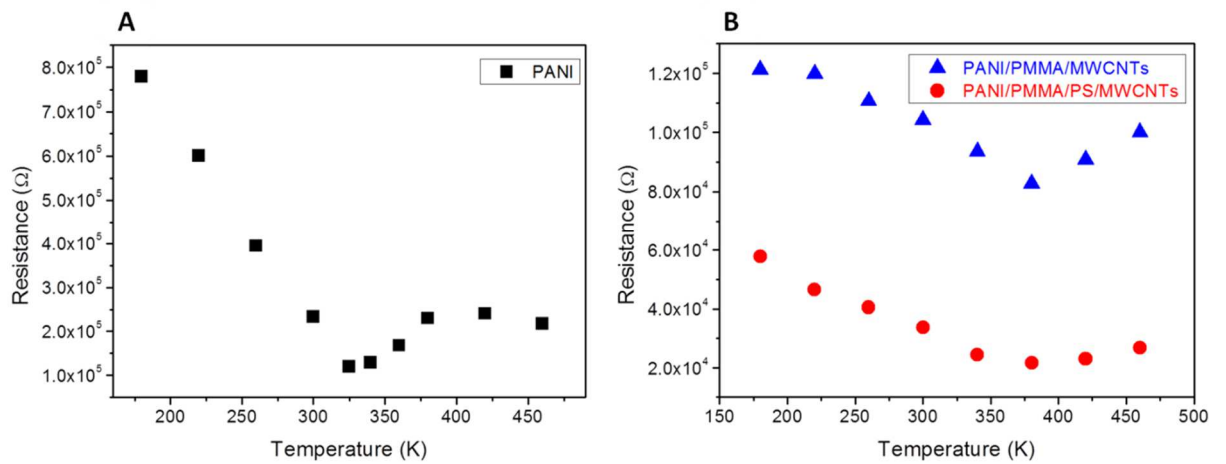


Fig. 4: Temperature dependence of the resistance for both PANI and PANI composites.

The decrease in resistance in the range 180 K - 325 K, for PANI, is more pronounced since the resistance decrease by factor 6.5 more than in the composite where it is only by a factor 1.5 and 2.5 for the PANI/PMMA/MWCNTs and PANI/PMMA/PS/MWCNTs respectively. Overall, the results show that this material and its composites present simultaneously a positive and negative temperature coefficient resistance (TCR) [62]. In such a case it is difficult to find out one model which fits perfectly to explain the resistance evolution.

Such behavior where both the positive and negative variation of the TCR existed simultaneously was already observed in previous studies [63-64] involving PANI-CSA (camphor sulfonic acid) or in PANI/PMMA blends [65]. The positive TCR is believed to arise from carriers scattering along the chains by phonons [62] and indicated a metallic nature. Long et al. [62] proposed a mix of metallic and non-metallic conduction mechanisms as responsible for such resistance evolution inversion (positive and negative evolution). The mechanisms associated with this mix are probably the metallic

conduction and conduction through a hopping mechanism. Lee et al. [66] have also observed this phenomenon in polyaniline/sulfonated polycarbonate blends. In fact, mixed metallic and non-metallic behavior is often observed as a characteristic of conducting polymers [67].

In the temperature range from 180 K to 360 K, the composites films show negative dR/dT indicative of nonmetallic behavior, while in the temperature range 360 K - 460 K the films show positive dR/dT indicative of metallic behavior [68]. This confirms a system composed of mixed metallic-nonmetallic character in terms of conductivity.

It is also worth noting that PMMA as an insulating matrix is used here to improve mechanical stability. But besides improving mechanical stability of PANI composites, the PMMA helps also in reducing the barriers to conductivity around the PANI particles and by way enhanced the conductivity [69-70]. Kaiser *et al.* [67] have also reported such a phenomenon and noticed that the blends are quite conductive. He explained this by the possibility for PANI to form PANI-rich seams running through the insulating host matrix [67]. After this electrical characterization we have found useful to explore the sensing performances associated with these electrical properties.

3. 5. Sensing performance evaluation.

3. 5. 1 Sensors response to ammonia.

Fig. 5 presents the typical response-recovery characteristics recorded at room temperature for PANI-based composites upon exposure to different concentrations of NH_3 ranging from 50 to 600 ppm. For comparison, the data corresponding to PMMA/MWCNTs (for the 10 wt% contents, but lower concentrations MWCNTs (7 wt%) are given in Fig. S2 in supporting information for more details), PANI/PS and PANI/PMMA/PS from 100 to 600 ppm are also displayed.

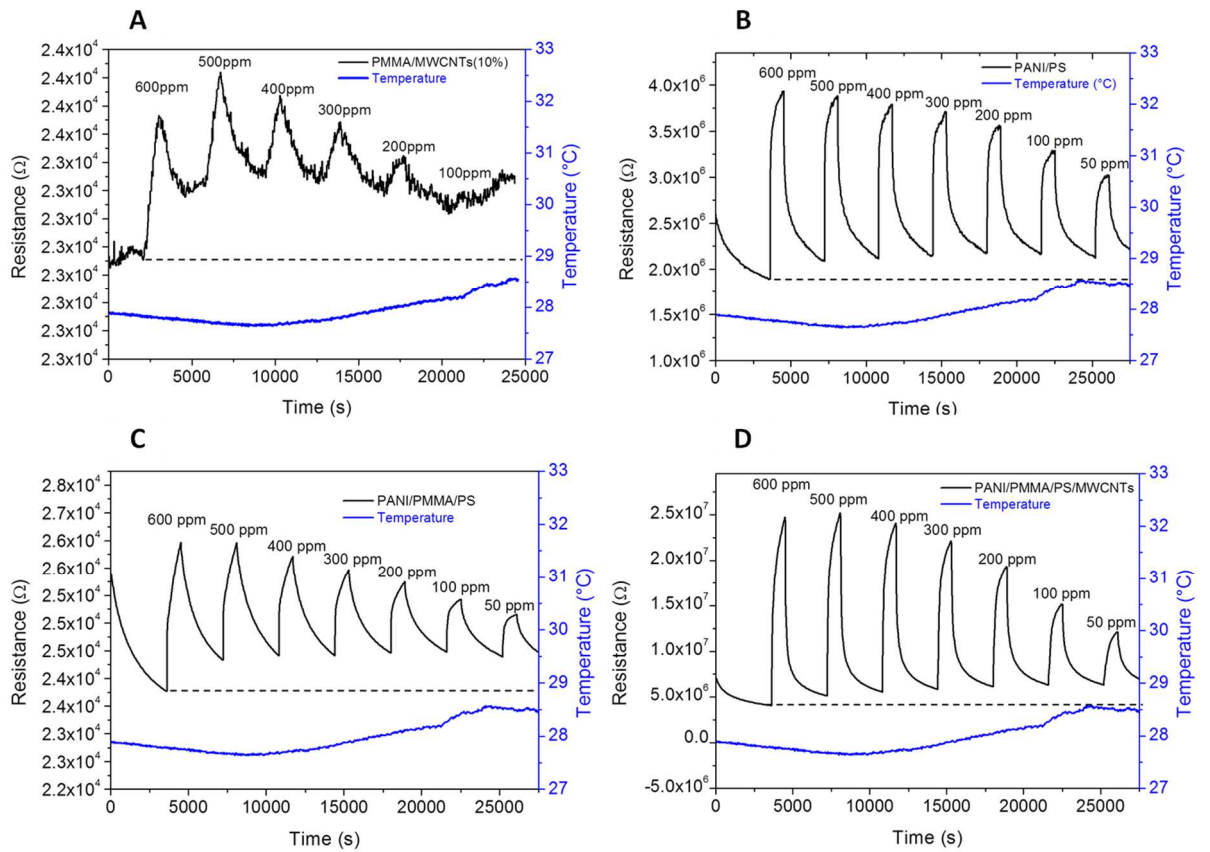


Fig. 5: Sensor response recorded at room temperature ($\sim 28^{\circ}\text{C}$) and RH of 4%: for (a) PANI/MWCNTs, (b) PANI/PS, (c) PANI/PMMA/PS and (d) PANI/PMMA/PS/MWCNTs towards ammonia gas (50-600 ppm).

For all sensors, the resistance immediately increased up upon exposure to ammonia gas. While for the PANI-based materials, the sensors more less reach promptly the steady-state, for the PMMA/MWCNTs the steady-state is not achieved. This can be attributed to the absence of PANI which is the most sensitive element in the reaction with ammonia. During exposure, the NH_3 molecules adsorb onto the surface of the PANI composite and react with PANI aggregates via deprotonation and this reaction results in the formation of ammonium ions. Since protonation ensures the doping of the PANI, reaction with NH_3 which consumes proton is the reverse reaction i.e. undoping and leads to resistance increase.

Recovery to baseline resistance is only partially attained after the first exposure for the PANI-Based composites. This behaviour can be explained by focusing on the first exposure cycle. In fact, during the first exposure to ammonia gas, the sensor surfaces will offer all available interaction sites. While most of the interactions sites experience reversible adsorption/desorption reactions, some interactions sites are subjected to irreversible chemical reactions (with gaseous species or moisture). These reactions lead

to uncompleted desorption during the first sweeping of the sensor surface by purified air. And since those interaction sites (subjected to irreversible chemical reactions) have been mostly involved during the first exposure cycle they are less active in the following cycles. Having a look at Fig. S6 in the supporting information, it should be noted that the sensor seems also to experience baseline resistance variation due to temperature fluctuation which could explain also the baseline drift. However, we have not found a real correlation between temperature fluctuation and the baseline resistance under dynamic exposure/air zero cleaning sequences (see temperature evolution in Fig. 5).

As announced earlier, to improve electrical properties and therefore sensitivity of sensor, multi-walled carbon nanotubes (MWCNTs) are added to the composite. It should be noticed that MWCNTs alone (embedded in PMMA) as presented in Fig. 5a do not display interesting features. In contrast, the presence of PANI, as presented in Fig. 5b-d provided a good and stable response. This means that PANI itself in these composites plays an important role in the detection of ammonia. In fact, as already observed and reported, PANI is well suited for the detection of ammonia. An example of ammonia detection using only PANI is shown in Fig. S3a (see supporting information). The importance of PANI is confirmed through Fig. 5b and 5c where a sensitive and reversible signal is obtained for PS/PANI and PS/PMMA/PANI. To understand the role played by both PANI and MWCNTs when embedded in a PS/PMMA polymer matrix we can focus on Fig. 5d. Here again, we observed a sensitive and reversible signal with a larger resistance variation compared to the previous examples. This improvement is attributed to the presence of MWCNTs which combined to the PANI allow increasing the conduction path through the insulating matrix. Working with this concentration of MWCNTs (3.5 wt%) is an optimum since the composite where the MWCNTs contain is higher (7 wt%) present lower response (see Fig. S3b in the supporting information).

Fig. 6 represents the calibration curves for PANI composites. In this figure, the responses are given as relative resistance variation ($\Delta R/R_0$) (ΔR) (but responses in the form of relative resistance given in is available in Fig. S4 in the supporting information). For clarity, the calibration curves of PMMA/MWCNTs and PANI/PMMA/MWCNTs are not represented. Here again the PANI/PMMA/PS/MWCNTs present the most important slope confirming the best performance of this composite.

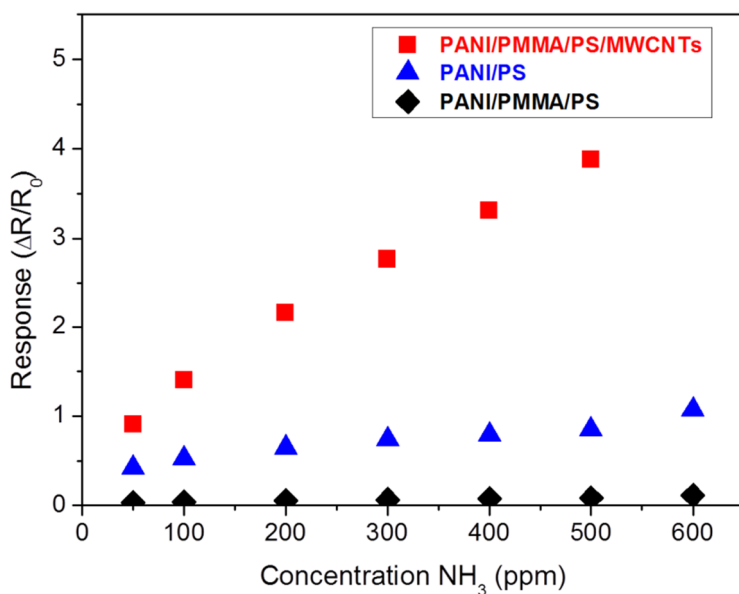


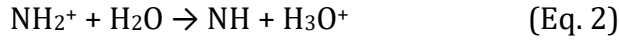
Fig. 6: Calibration curves for PANI/PS, PANI/PMMA/PS and PANI/PMMA/PS/MWCNTs as function of NH₃ concentration, measured at room temperature (~28°C) and RH of 4%.

All the composites, PS/PANI, PS/PMMA/PANI and PANI/PMMA/PS/MWCNTs present a rather linear response characterized by their linearization coefficients (R^2) of 0.953 and 0.972, and 0.982 respectively. However, a deep analysis of the calibration curve of the shows two slopes: a stronger linear slope from 50 to 300 ppm, and another portion (from 300 to 600 ppm) with a rather weaker linear slope. The first portion is characterized by larger resistance variation between the consecutive concentrations while the second portion is characterized by a smaller resistance variation between the consecutive concentrations. If the first portion corresponds to the concentration range where the sensor response gives a linear feature the second portion can be attributed to a sort of saturation when NH₃ concentrations is laying in the higher concentrations range.

3.5.2 Humidity effect on the NH₃-sensing and cross sensitivity of the composite.

Fig. 7 shows the humidity responses of PANI composites exposed to 300 ppm of NH₃ while varying the relative humidity (RH) from 10 to 70%. For clarity, the results of PANI itself are also incorporated for the discussion. The effect of humidity is attributed to the proton exchange mechanism between the polymer and the adsorbed water vapor on the surface. In fact, upon ammonia exposure in humid conditions, there is a

competition between H₂O and NH₃ to interact with proton on the surface of polyaniline. This transfer competition can be described by the following acid-base reactions [71]:



The first equation consists of a proton consuming from the PANI (-NH⁺) matrix and gives rise to resistance increase i.e. conductivity decreases while the second equation is a proton release from the leuco-emeraldine (-NH₂⁺) salt and gives rise to conductivity increase [71].

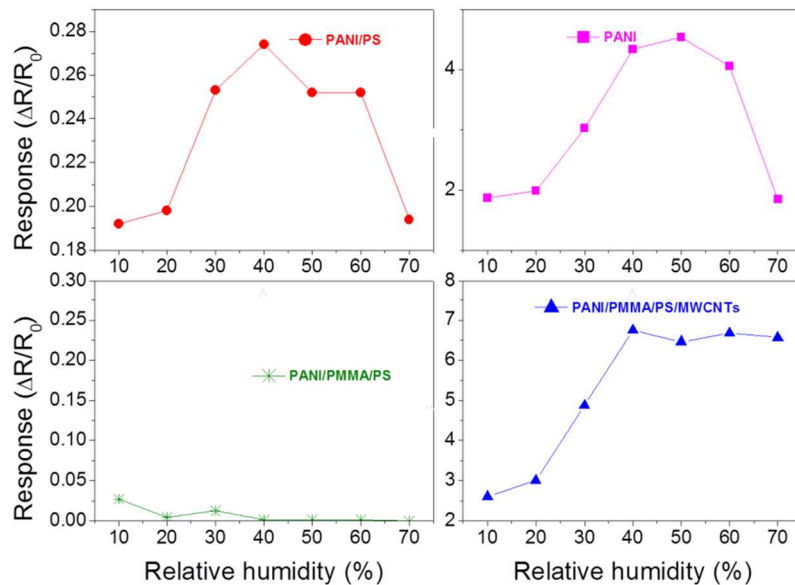


Fig. 7: Sensors responses to 300 ppm of NH₃ exposure at various relative humidity percentage for PANI composites and PANI measured at room temperature (~28°C).

In this figure, we can see that, apart from PANI that experience an increase of the responses until 50% of relative humidity, for all the other displayed sensors, the responses slightly increase until 40% of relative humidity. Above 40% of RH for PANI/PS, and above 50% for PANI, the responses decrease while the PANI/PMMA/PS/MWCNTs composite tends to stabilize until higher humidity levels. The increase of the response within 10-40% of RH is attributed to a combined action of NH₃ (deprotonation = resistance increase) on the PANI and swelling (reduction of the conduction path) of the polymer matrix with a domination of the equation 1. After 40% of RH, the response of the PANI/PS composite and PANI decreases continuously as the relative humidity increases. In this case, even if deprotonation by NH₃ and the swelling

(leading both to increase of the resistance) are important, the resulting resistance increase is counterbalanced by the resistance decrease as a result of the transformation from the leuco-emeraldine salt (proton release) as given in equation 2 and gives rise to a conductivity increase. This means that even if the two reactions are in competition, at a higher level of humidity the equation 2 should dominate and is certainly favored by the H₂O introduction.

The result can be surprising for PANI/PS since PS is known for its hydrophobicity. However looking at the SEM picture where the PS forms sphere-like particles with PANI, we can imagine that the sensor films does not form a compact film and that PANI is not well embedded into the PS matrix to form a stable film which can limit the humidity action. This is further confirmed by the evolution of the response upon increasing the humidity in Fig. 7. For PANI/PMMA/PS/MWCNTs composite the response is relatively stable at higher humidity level showing an acceptable behavior to humidity action. This is the result of the stable film in which swelling is limited. We can see that, while the sensor response of PANI/PMMA/PS/MWCNTs tends to stabilize as the relative humidity increases, it continues decreasing for PANI alone, leading to a loss in the response. For the PANI/PMMA/PS a dramatic loss of sensitivity has been observed to that point that the sensor was even not usable after this experiment. It should be noted also that upon diffusion of NH₃ molecules into the polymer, the conduction paths can be hindered by swelling and this will result on the loss of electrical properties. Humidity influence on PANI has been reported in early studies in which authors have shown that the presence of water molecules enhance the conductivity of PANI [72-73].

Having a look at the transient resistance response of the composite (Fig. S4 in the supporting information) allows seeing that the incomplete recovery is less accentuated in humidified conditions. As we already mentioned in section 3.5.1, some interactions sites are subjected to irreversible chemical reactions (with gaseous species or moisture). In humidified conditions, the film is less moisture sensitive since the chamber is saturated with water molecules. Therefore, the sensor baseline is less sensitive to incomplete recovery. We have also observed that the response time under ammonia exposure in a humid environment was slightly higher than in dried condition (see the following section). The response time and recovery time at 30% RH under 300 ppm NH₃, for example, were estimated to 360 sec and 690 sec respectively. This increase in

kinetics of adsorption and desorption is also attributed to the competition between NH_3 and water.

3.5.3 Sensor performance in the lower concentration range: stability, repeatability and cross sensitivity of the composite.

As the sensor response gives a linear response in the range under 200 ppm as displayed in the calibration curve of Fig. 7, we focus on the lower concentration range to study the performances of the PANI/PMMA/PS/MWCNTs as being the most sensitive sensors over all the composites. In this experiment, we performed gas sensing exposures between 5 and 20 ppm and we also tested the stability and repeatability of the composite in this same range. The results are presented in Fig. 8.

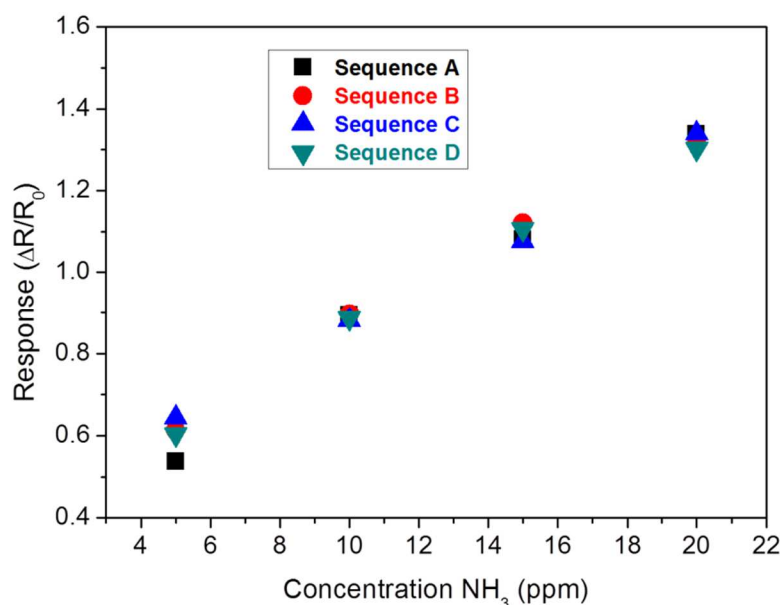


Fig. 8: Sensor response to four sequences of exposure of NH_3 in the lower concentration range (5 – 20 ppm) for the PANI/PMMA/PS/MWCNTs composite, measured at room temperature ($\sim 28^\circ\text{C}$) and RH of 4.5%.

Here we performed sequences by increasing the NH_3 concentration (5-->10-->15-->20 ppm: sequences A and C) and by decreasing the NH_3 concentration in a disordered way (20-->10-->15-->5 ppm: sequences B and D) to check the linearity and hysteresis. An example of sensor response to ammonia exposure (sequence A) for the composite PANI/PMMA/PS/MWCNTs is given in Fig. S5 in the supporting information. We can see in Fig. 8 that the sensor presents very good stability after 4 sequences of increasing and decreasing concentration. The responses are quite repeatable independently of the

exposure sequences. This stability of the sensor (PANI/PMMA/PS/MWCNTs) and the repeatability of its response is of course attributed to the presence of PANI and MWCNTs but also to the mechanical stability provided by the presence of PMMA and PS [74-77]. The PANI/PMMA/PS/MWCNTs presents a sensitivity of 162 k Ω /ppm (corresponding to 5%/ppm) within the 5 - 20 ppm range with a limit of detection (LOD) (using the 3S method: LOD=3xSD/slope; SD: standard deviation) averaging 830 ppb. The response time and recovery time at 20 ppm were estimated (from Fig. S5) at 270 sec and 630 sec, respectively.

Besides sensitivity, selectivity or cross-sensitivity is also an important parameter for checking the performance of gas sensors. Therefore the cross-sensitivity of the PANI/PMMA/PS/MWCNTs composite has also been investigated and the result presented in Fig. 9.

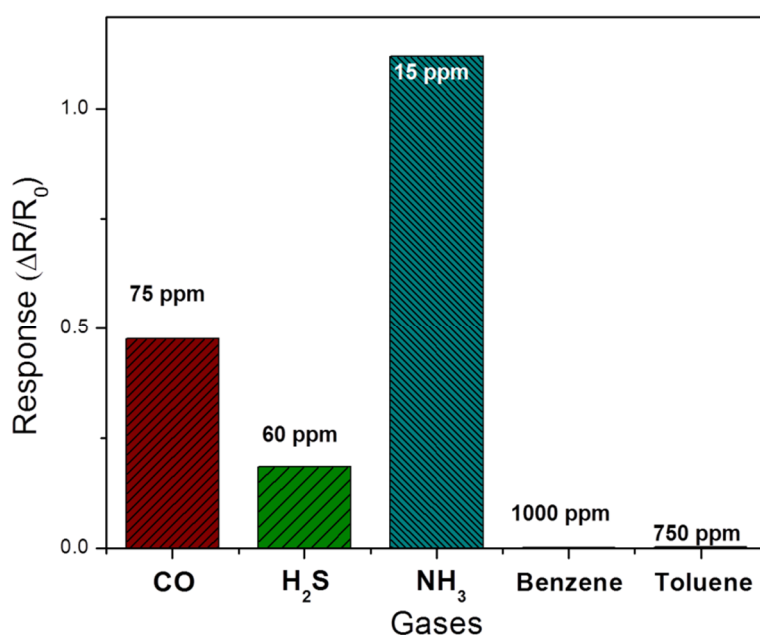


Fig. 9: Selectivity histogram of composite film sensor (PANI/PMMA/PS/MWCNTs) toward different gases at room temperature ($\sim 28^\circ\text{C}$) and RH of 4.5%.

Fig. 9 shows the cross-sensitivity histogram of the composite film toward different gases (carbon monoxide (CO), hydrogen sulfide (H₂S), ammonia (NH₃), benzene and toluene). The sensor film exhibits clearly a partial selective response for ammonia and negligible response toward a higher concentration of other volatile organic compounds (benzene and toluene). For the other interfering gases, H₂S and

NH₃, they can potentially interfere with ammonia in the lower concentration range only if their concentration is higher than the reported (> 60 ppm for H₂S, and > 75 ppm for CO). We have also tested the PANI-PMMA-PS-MWCNT composite, to nitrogen oxide (NO₂) which is a strong oxidizing gas. However the results (Fig. S7 in the supporting information) seem to confirm a very weaker sensitivity and the resistance variation are difficult to calculate to be include here. However, globally, the composite sensor presents a higher sensor response compared to interfering gases.

Finally, the PANI-PMMA-PS-MWCNT composite is compared to other PANI-based composites able to detect NH₃. The results are gathered in Table 1, and for the clarity, we delimited the comparison with composites (PANI /polymers) or hybrids (PANI /CNTs) materials that fit best to our example. We can depict from this table that our composite presents very good performances compared to the already published works in this field of PANI-based composite sensors. In both the response time and recovery time as well as responses in the lower concentration range, we present acceptable performances. In this table, the term "response (%) at x ppm" means the response calculated as $\Delta R/R_0$ (given in %) at x (given concentration value) in ppm.

Table 1: Comparison of the composite sensor performance to other PANI blends-based sensors for NH₃ detection.

Material	Detection range (ppm)	Response (%) at x ppm	Sensitivity (%/ppm)	τ_{resp} (sec)	τ_{rec} (sec)	RH (%)	Reference
PANI/MWCNTs	0.2 - 150	100% at 75 ppm	NA	22	202	NA	[20]
PANI/MWCNTs	0.5 - 290	320% at 100 ppm	0.9	1200	2400	NA	[78]
PANI/PMMA	1-100	550% at 30 ppm	27	200	300	NA	[34]
PANI/PMMA	800-2400	11% ^{b)} at 800 ppm	27.8 ^{c)}	22	400	NA	[79]
PANI/PS	100 ^{a)}	200% at 100 ppm	NA	600	NA	NA	[35]
PANI/PEO	0.5 - 100	600% at 100 ppm	NA	420 - 1020	300 - 1080	NA	[80]
PANI/PMMA/PS/MWCNTs	1 - 20	134% at 20 ppm	5	270	630	10-70	This work

a) Exposure at 100ppm; b) response given as R/R_0 ; c) sensitivity at 42 °C; NA: not Available

In this table, the polyaniline/PMMA present sensitivity of 27%/ppm compared to 5%/ppm for our composite [34]. However, having a look at the morphology of the align

polyaniline/PMMA [34] allows seeing that in this case, the polymer matrix is a fibers-like structure that ensures a clear gain in the surface area giving rise to higher sensitivity and rapid kinetics. This is not the case in our film composite forming a smooth surface on which fibers are embedded. Such a surface state (with fibers embedded on the polymers) does not favour gain in surface area. However, our composite with response averaging 134% for 20 ppm, demonstrated better response for the detection of ammonia than that of sensors prepared using conventional mixing synthesis procedure [20, 34-35, 78-80] where responses are 100% at 75 ppm for PANI/MWCNTs, 200% at 100 ppm for PANI/PS, and 600% at 100 ppm PANI/PEO.

For the response and recovery time, PANI/MWCNTs [20] and PANI/PMMA [79] in this table present better values than our composite. This is partly explained, in the case of PANI/MWCNTs [20], by the in-situ polymerization method which allows to perfectly cover the MWCNTs surfaces and ensuring rapid kinetics. While for the PANI/PMMA [79], even if the synthesis procedure based on electrospinning and in situ polymerization allows to get stable structure, the operating temperature at 42° C can explain the rapid kinetics. It would be interesting to evaluate the sensing performance under a humid environment, unfortunately, its influence on the sensors has not been reported in these studies [20, 34-35, 78-80]. The performance of our sensors in the lower detection region, below the TLV for long and short term exposure, associated with the linearity of the calibration curve and the stability in a humid environment is clearly promising issues for future applications.

3.5.4 Long-term stability studies of the PANI-PMMA-PS-MWCNT composite.

Besides sensing performance studied above, long-term stability is another important parameter for checking the performance of gas sensors. The long-term stability of the composite sensor has been evaluated through analyzing the resistance variation under ammonia gas from 600 ppm to 50 ppm. To this end, six similar cycles of exposure have been made within 4 weeks. Fig. 10 shows the results of this study and the corresponding responses are given in Fig. S8 in the supporting information.

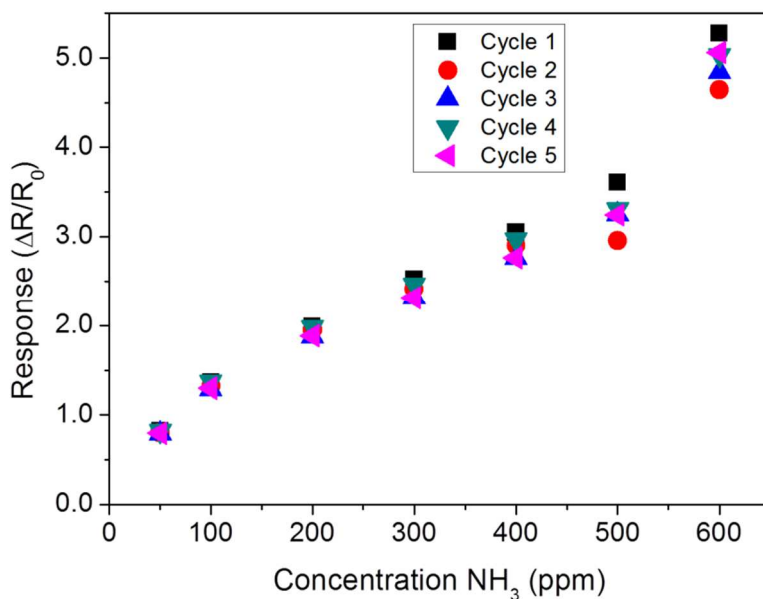


Fig. 10: Sensor response to many cycles of exposure of NH₃ (50 – 600 ppm) for the PANI/PMMA/PS/MWCNTs composite, measured at room temperature (~28°C) and RH of 4.5%.

The analysis of the response evolution along the exposure cycles underlines acceptable long-term stability at lower concentration (< 300 ppm) while at the higher concentration (> 300 ppm) a slight deviation is observed. However, we can notice that the sensor responses globally satisfy the long-term stability tests. This observation is an important point showing that apart from the good result in a humid environment, the composite film also satisfies long-term stability making this material and the synthesis way a prominent way for our future application. As we have seen in this study the lower the concentration used the more reliable the response in the long-term period. Therefore, we can assume that long-term stability might be improved if the sensors are exposed only to a lower concentration range. It is also worth noting that with this study, the repeatability of sensor response can be once more evidenced.

Even if adding other polymers to PANI is a good way to realize sensitive and stable films in humid environment, the right combination of these elements with a filler such as MWCNTs is essential. However, using a specific synthesis protocol seems to play a crucial role for the formation of sensitive and stable sensor film while keeping the role of PANI in the composite.

6. Conclusion

In this paper, we have prepared PANI composites based on the use of PMMA and PS blends. The addition of MWCNTs to this matrix has shown that these later are able to improve the conductivity of the composites by creating a conduction path through the polymer matrix. The presence of PS/PMMA improves mechanical stability while simultaneously limiting the humidity action. It comes out that the PANI/PMMA/PS/MWCNTs presents the best sensor performances for NH₃ detection over all the composites. Furthermore, it presents very good stability and repeatability. The PS-PMMA-MWCNT-PANI composite presents a lower detection limit averaging 830 ppb and shorter response time and recovery time at 20 ppm averaging 270 sec and 630 sec respectively. The success of this preparation is attributed to the synthesis way which alternates heating and ultrasonic treatment. The good sensor performances recorded are attributed to the combined action of all the elements composing this composite and the stability in a humid environment is a result of such synergetic effect.

Acknowledgement

This work was sponsored by a public grant overseen by the French National Research Agency as part of the "Investissements d'Avenir" through the IMobS³ Laboratory of Excellence (ANR-10-LABX-0016) and the IDEX-ISITE initiative CAP 20-25 (ANR-16-IDEX-0001).

Supporting Information

The Supporting Information is available free of charge on the website. The file contains preparation details of the sensor composites, SEM image of the PMMA/MWCNTs, sensor response to ammonia for the PANI/MWCNTs (7 wt%), sensor response to ammonia for PANI and PANI/PMMA/PS/MWCNTs (7 wt%), sensor response to ammonia et different humidity levels, sensors response of the composite in the low concentration range, typical resistance evolution of the sensor under air zero as function of operating temperature, sensor response to NO₂, and sensor response to many cycles of ammonia exposure for the long-term stability experiments.

REFERENCES

[1] Z. Song, Z. Wei, B. Wang, Z. Luo, S. Xu, W. Zhang, et al., Sensitive Room-Temperature H₂S Gas Sensors Employing SnO₂ Quantum Wire/Reduced Graphene Oxide Nanocomposites, *Chem. Mater.* 28(2016) 1205-12.

- [2] D.D. Trung, N.D. Cuong, K.Q. Trung, T.-D. Nguyen, N. Van Toan, C.M. Hung, et al., Controlled synthesis of manganese tungstate nanorods for highly selective NH₃ gas sensor, *J. Alloys Compd.* 735(2018) 787-94.
- [3] A. Paliwal, A. Sharma, M. Tomar, V. Gupta, Carbon monoxide (CO) optical gas sensor based on ZnO thin films, *Sens. Actuators, B* 250(2017) 679-85.
- [4] L. Sun, W. Fang, Y. Yang, H. Yu, T. Wang, X. Dong, et al., Highly active and porous single-crystal In₂O₃ nanosheet for NO_x gas sensor with excellent response at room temperature, *RSC Adv.* 7(2017) 33419-25.
- [5] K.-P. Yoo, K.-H. Kwon, N.-K. Min, M.J. Lee, C.J. Lee, Effects of O₂ plasma treatment on NH₃ sensing characteristics of multiwall carbon nanotube/polyaniline composite films, *Sens. Actuators, B* 143(2009) 333-40.
- [6] Toxicological profile for Ammonia, U.S. Department of Health and Human Services, Agency for Toxic Substances and Disease Registry (ATSDR), Atlanta, GA, 2004.
- [7] P. Kjeldsen, M.A. Barlaz, A.P. Rooker, A. Baun, A. Ledin, T.H. Christensen, Present and Long-Term Composition of MSW Landfill Leachate: A Review, *Crit. Rev. Environ. Sci. Technol.* 32(2002) 297-336.
- [8] Burak YUZER, Deniz AKGUL, B. MERTOGLU, Effect of High Ammonia Concentration on UASB Reactor Treating Sanitary Landfill Leachate, *Marmara Univ. Fen Bilimleri Derg.* 24(2012) 59-67.
- [9] R. Shamsi, M. Mahyari, M. Koosha, Synthesis of CNT-polyurethane nanocomposites using ester-based polyols with different molecular structure: Mechanical, thermal, and electrical properties, *J. Appl. Polym. Sci.* 134(2017).
- [10] S. Stankovich, D.A. Dikin, G.H.B. Dommett, K.M. Kohlhaas, E.J. Zimney, E.A. Stach, et al., Graphene-based composite materials, *Nature*, 442(2006) 282-6.
- [11] S. Li, P. Lin, L. Zhao, C. Wang, D. Liu, F. Liu, et al., The room temperature gas sensor based on Polyaniline@flower-like WO₃ nanocomposites and flexible PET substrate for NH₃ detection, *Sens. Actuators, B* 259(2018) 505-13.
- [12] C. Liu, H. Tai, P. Zhang, Z. Yuan, X. Du, G. Xie, et al., A high-performance flexible gas sensor based on self-assembled PANI-CeO₂ nanocomposite thin film for trace-level NH₃ detection at room temperature, *Sens. Actuators, B* 261(2018) 587-97.
- [13] D. Zhang, Z. Wu, P. Li, X. Zong, G. Dong, Y. Zhang, Facile fabrication of polyaniline/multi-walled carbon nanotubes/molybdenum disulfide ternary nanocomposite and its high-performance ammonia-sensing at room temperature, *Sens. Actuators, B* 258(2018) 895-905.
- [14] B.S. Sherigara, W. Kutner, F. D'Souza, Electrocatalytic Properties and Sensor Applications of Fullerenes and Carbon Nanotubes, *Electroanalysis*, 15(2003) 753-72.
- [15] J.B. Bai, A. Allaoui, Effect of the length and the aggregate size of MWNTs on the improvement efficiency of the mechanical and electrical properties of nanocomposites—experimental investigation, *Composites Part A* 34(2003) 689-94.
- [16] S. Xie, W. Li, Z. Pan, B. Chang, L. Sun, Mechanical and physical properties on carbon nanotube, *J. Phys. Chem. Solids* 61(2000) 1153-8.
- [17] M. Zaki, M. Nasir, U. Hashim, M.K.M. Arshad, Characterization of difference carbon nanotubes (CNTs) as a sensing mechanism for development of formaldehyde gas detection sensor, *IEEE Reg. Symp. Micro Nanoelectron.* (2017) 179-82.
- [18] D. Kumar, P. Chaturvedi, P. Saho, P. Jha, A. Chouksey, M. Lal, et al., Effect of single wall carbon nanotube networks on gas sensor response and detection limit, *Sens. Actuators, B* 240(2017) 1134-40.
- [19] Md.Masud Rana, Dauda Sh. Ibrahim, M.R. Mohd Asyraf, S. Jarin, A. Tomal, A review on recent advances of CNTs as gas sensors, *Sens. Rev.* 37(2017) 127-36.
- [20] L. He, Y. Jia, F. Meng, M. Li, J. Liu, Gas sensors for ammonia detection based on polyaniline-coated multi-wall carbon nanotubes, *Mater. Sci. Eng., B* 163(2009) 76-81.
- [21] J. Kong, N.R. Franklin, C. Zhou, M.G. Chapline, S. Peng, K. Cho, et al., Nanotube Molecular Wires as Chemical Sensors, *Science*, 287(2000) 622-5.

- [22] P.-C. Ma, M.-Y. Liu, H. Zhang, S.-Q. Wang, R. Wang, K. Wang, et al., Enhanced Electrical Conductivity of Nanocomposites Containing Hybrid Fillers of Carbon Nanotubes and Carbon Black, *ACS Appl. Mater. Interfaces*, 1(2009) 1090-6
- [23] H. Han, S. Cho, Fabrication of Conducting Polyacrylate Resin Solution with Polyaniline Nanofiber and Graphene for Conductive 3D Printing Application, *Polymers*, 10(2018) 1003.
- [24] N.R. Tanguy, M. Thompson, N. Yan, A review on advances in application of polyaniline for ammonia detection, *Sens. Actuators, B* 257(2018) 1044-64..
- [25] R.V. Salvatierra, G. Zitzer, S.A. Savu, A.P. Alves, A.J.G. Zarbin, T. Chassé, et al., Carbon nanotube/polyaniline nanocomposites: Electronic structure, doping level and morphology investigations, *Synth. Met.* 203(2015) 16-21.
- [26] A.G. MacDiarmid, "Synthetic Metals": A Novel Role for Organic Polymers (Nobel Lecture), *Angew. Chem., Int. Ed.* 40(2001) 2581-90.
- [27] A. Roy, A. Ray, S. Saha, S. Das, Investigation on energy storage and conversion properties of multifunctional PANI-MWCNT composite, *Int. J. Hydrogen Energy* 43(2018) 7128-39.
- [28] H. Tai, Y. Jiang, G. Xie, J. Yu, X. Chen, Fabrication and gas sensitivity of polyaniline–titanium dioxide nanocomposite thin film, *Sens. Actuators, B* 125(2007) 644-50.
- [29] M. Ding, Y. Tang, P. Gou, M.J. Reber, A. Star, Chemical Sensing with Polyaniline Coated Single-Walled Carbon Nanotubes, *Adv. Mater.* 23(2011) 536-40.
- [30] M. Tabellout, K. Fatyeyeva, P.Y. Baillif, J.F. Bardeau, A.A. Pud, The influence of the polymer matrix on the dielectric and electrical properties of conductive polymer composites based on polyaniline, *J. Non-Cryst. Solids* 351(2005) 2835-41.
- [31] S. Srivastava, S.S. Sharma, S. Kumar, S. Agrawal, M. Singh, Y.K. Vijay, Characterization of gas sensing behavior of multi walled carbon nanotube polyaniline composite films, *Int. J. Hydrogen Energy* 34(2009) 8444-50.
- [32] A. Roy, A. Ray, P. Sadhukhan, K. Naskar, G. Lal, R. Bhar, et al., Polyaniline-multiwalled carbon nanotube (PANI-MWCNT): Room temperature resistive carbon monoxide (CO) sensor, *Synth. Met.* 245(2018) 182-9.
- [33] S. Abdulla, T.L. Mathew, B. Pullithadathil, Highly sensitive, room temperature gas sensor based on polyaniline-multiwalled carbon nanotubes (PANI/MWCNTs) nanocomposite for trace-level ammonia detection, *Sens. Actuators, B* 221(2015) 1523-34.
- [34] H.-D. Zhang, C.-C. Tang, Y.-Z. Long, J.-C. Zhang, R. Huang, J.-J. Li, et al., High-sensitivity gas sensors based on arranged polyaniline/PMMA composite fibers, *Sens. Actuators, A* 219(2014) 123-7.
- [35] L.-Y. Yang, W.-B. Liao, Environmental responses of nanostructured polyaniline films based on polystyrene–polyaniline core–shell particles, *Mater. Chem. Phys.* 115(2009) 28-32.
- [36] L. Al-Mashat, K. Shin, K. Kalantar-zadeh, J.D. Plessis, S.H. Han, R.W. Kojima, et al., Graphene/Polyaniline Nanocomposite for Hydrogen Sensing, *J. Phys. Chem. C* 114(2010) 16168-73.
- [37] S. Srivastava, S.S. Sharma, S. Agrawal, S. Kumar, M. Singh, Y.K. Vijay, Study of chemiresistor type CNT doped polyaniline gas sensor, *Synth. Met.* 160(2010) 529-34.
- [38] N.N. Rozik, A.I. Khalaf, A.A. Ward, Studies the behaviors of polyaniline on the properties of PS/PMMA blends, *Proc. Inst. Mech. Eng., Part L* 230(2016) 526-36.
- [39] Y. Li, J.Q. Pham, K.P. Johnston, P.F. Green, Contact Angle of Water on Polystyrene Thin Films: Effects of CO₂ Environment and Film Thickness, *Langmuir*, 23(2007) 9785-93.
- [40] M. Matsuguchi, A. Okamoto, Y. Sakai, Effect of humidity on NH₃ gas sensitivity of polyaniline blend films, *Sens. Actuators, B* 94(2003) 46-52.
- [41] J. Guo, N. Briggs, S. Crossley, B.P. Grady, Morphology of polystyrene/poly(methyl methacrylate) blends: Effects of carbon nanotubes aspect ratio and surface modification, *AIChE J.* 61(2015) 3500-10.
- [42] E. Segal, Y. Haba, M. Narkis, A. Siegmann, On the structure and electrical conductivity of polyaniline/polystyrene blends prepared by an aqueous-dispersion blending method, *J. Polym. Sci., Part B: Polym. Phys.* 39(2001) 611-21.
- [43] S. Ji, Y. Li, M. Yang, Gas sensing properties of a composite composed of electrospun poly(methyl methacrylate) nanofibers and in situ polymerized polyaniline, *Sens. Actuators, B* 133(2008) 644-9.

- [44] H. Liu, J. Kameoka, D.A. Czaplewski, H.G. Craighead, Polymeric Nanowire Chemical Sensor, *Nano Lett.* 4(2004) 671-5.
- [45] S.Y. Hobbs, M.E.J. Dekkers, V.H. Watkins, Effect of interfacial forces on polymer blend morphologies, *Polymer*, 29(1988) 1598-602.
- [46] S. Ravati, B.D. Favis, Low percolation threshold conductive device derived from a five-component polymer blend, *Polymer*, 51(2010) 3669-84.
- [47] E. Zampetti, A. Muzyczuk, A. Macagnano, S. Pantalei, S. Scalese, C. Spinella, et al., Effects of temperature and humidity on electrospun conductive nanofibers based on polyaniline blends, *J. Nanopart. Res.* 13(2011) 6193-200.
- [48] M. Joulazadeh, A.H. Navarchian, M. Niroomand, A Comparative Study on Humidity Sensing Performances of Polyaniline and Polypyrrole Nanostructures, *Adv. Polym. Technol.* 33(2014) 21461.
- [49] F. Gu, X. Yin, H. Yu, P. Wang, L. Tong, Polyaniline/polystyrene single-nanowire devices for highly selective optical detection of gas mixtures, *Opt. Express*, 17(2009) 11230-5.
- [50] A. Macagnano, V. Perri, E. Zampetti, A. Bearzotti, F. De Cesare, Humidity effects on a novel eco-friendly chemosensor based on electrospun PANi/PHB nanofibres, *Sens. Actuators, B* 232(2016) 16-27.
- [51] M. Farbod, S. Khajepour Tadavani, Electrical properties and glass transition temperature of multiwalled carbon nanotube/polyaniline composites, *J. Non-Cryst. Solids* 358(2012) 1339-44.
- [52] K. Pandey, P. Yadav, I. Mukhopadhyay, Elucidating the effect of copper as a redox additive and dopant on the performance of a PANI based supercapacitor, *Phys. Chem. Chem. Phys.* 17(2015) 878-87.
- [53] M. Trchová, J. Stejskal, Polyaniline: The infrared spectroscopy of conducting polymer nanotubes (IUPAC Technical Report), *Pure Appl. Chem.* 83(2011) 1803.
- [54] E.N. Konyushenko, J. Stejskal, I. Šeděnková, M. Trchová, I. Sapurina, M. Cieslar, et al., Polyaniline nanotubes: conditions of formation, *Polym. Int.* 55(2006) 31-9.
- [55] F. Yakuphanoglu, E. Basaran, B.F. Şenkal, E. Sezer, Electrical and Optical Properties of an Organic Semiconductor Based on Polyaniline Prepared by Emulsion Polymerization and Fabrication of Ag/Polyaniline/n-Si Schottky Diode, *J. Phys. Chem. B* 110(2006) 16908-13.
- [56] M.A.C. Mazzeu, L.K. Faria, M.R. Baldan, M.C. Rezende, E.S. Gonçalves, Influence of reaction time on the structure of polyaniline synthesized on a pre-pilot scale, *Braz. J. Chem. Eng.* 35(2018) 123-30.
- [57] Y. Furukawa, F. Ueda, Y. Hyodo, I. Harada, T. Nakajima, T. Kawagoe, Vibrational spectra and structure of polyaniline, *Macromolecules*, 21(1988) 1297-305.
- [58] Z. Ping, In situ FTIR-attenuated total reflection spectroscopic investigations on the base-acid transitions of polyaniline. Base-acid transition in the emeraldine form of polyaniline, *J. Chem. Soc., Faraday Trans.* 92(1996) 3063-7.
- [59] M.I. Boyer, S. Quillard, E. Rebourt, G. Louarn, J.P. Buisson, A. Monkman, et al., Vibrational Analysis of Polyaniline: A Model Compound Approach, *J. Phys. Chem. B* 102(1998) 7382-92.
- [60] J. Stejskal, I. Sapurina, M. Trchová, E.N. Konyushenko, Oxidation of Aniline: Polyaniline Granules, Nanotubes, and Oligoaniline Microspheres, *Macromolecules*, 41(2008) 3530-6.
- [61] M. Ahlskog, M. Reghu, A.J. Heeger, The temperature dependence of the conductivity in the critical regime of the metal - insulator transition in conducting polymers, *J. Phys.: Condens. Matter* 9(1997) 4145-56.
- [62] Y. Long, Z. Chen, N. Wang, J. Li, M. Wan, Electronic transport in PANI-CSA/PANI-DBSA polyblends, *Phys. B (Amsterdam, Neth.)* 344(2004) 82-7.
- [63] N.T. Kemp, G.U. Fianagan, A.B. Kaiser, H.J. Trodahl, B. Chapman, A.C. Partridge, et al., Temperature-dependent conductivity of conducting polymers exposed to gases, *Synth. Met.* 101(1999) 434-5.
- [64] B. Sixou, J.P. Travers, Y.F. Nicolau, Effect of aging induced disorder on transport properties of PANI-CSA, *Synth. Met.* 84(1997) 703-4.
- [65] M. Reghu, C.O. Yoon, C.Y. Yang, D. Moses, P. Smith, A.J. Heeger, et al., Transport in polyaniline networks near the percolation threshold, *Phys. Rev. B* 50(1994) 13931-41.

- [66] W.-J. Lee, Y.-J. Kim, S. Kaang, Electrical properties of polyaniline/sulfonated polycarbonate blends, *Synth. Met.* 113(2000) 237-43.
- [67] A.B. Kaiser, Systematic Conductivity Behavior in Conducting Polymers: Effects of Heterogeneous Disorder, *Adv. Mater.* 13(2001) 927-41.
- [68] E. Bekyarova, M.E. Itkis, N. Cabrera, B. Zhao, A. Yu, J. Gao, et al., Electronic Properties of Single-Walled Carbon Nanotube Networks, *J. Am. Chem. Soc.* 127(2005) 5990-5.
- [69] C.K. Subramaniam, A.B. Kaiser, P.W. Gilberd, C.J. Liu, B. Wessling, Conductivity and thermopower of blends of polyaniline with insulating polymers (PETG and PMMA), *Solid State Commun.* 97(1996) 235-8.
- [70] G.E. Collins, L.J. Buckley, Conductive polymer-coated fabrics for chemical sensing, *Synth. Met.* 78(1996) 93-101.
- [71] S. Jain, S. Chakane, A.B. Samui, V.N. Krishnamurthy, S.V. Bhoraskar, Humidity sensing with weak acid-doped polyaniline and its composites, *Sens. Actuators, B* 96(2003) 124-9.
- [72] S.C. Nagaraju, A.S. Roy, J.B.P. Kumar, K.R. Anilkumar, G. Ramagopal, Humidity Sensing Properties of Surface Modified Polyaniline Metal Oxide Composites, *J. Eng.* 2014(2014).
- [73] T. Taka, Humidity dependency of electrical conductivity of doped polyaniline, *Synth. Met.* 57(1993) 5014-9.
- [74] J. Lenis, S. Razavi, K.D. Cao, B. Lin, K.Y.C. Lee, R.S. Tu, et al., Mechanical Stability of Polystyrene and Janus Particle Monolayers at the Air/Water Interface, *J. Am. Chem. Soc.* 137(2015) 15370-3.
- [75] J. Zhu, P. Start, K.A. Mauritz, C.A. Wilkie, Thermal stability and flame retardancy of poly(methyl methacrylate)-clay nanocomposites, *Polym. Degrad. Stab.* 77(2002) 253-8.
- [76] K.C. Manikandan Nair, S. Thomas, G. Groeninckx, Thermal and dynamic mechanical analysis of polystyrene composites reinforced with short sisal fibres, *Compos. Sci. Technol.*, 61(2001) 2519-29.
- [77] T. Çaykara, O. Güven, UV degradation of poly(methyl methacrylate) and its vinyltriethoxysilane containing copolymers, *Polym. Degrad. Stab.* 65(1999) 225-9.
- [78] P. Lobotka, P. Kunzo, E. Kovacova, I. Vavra, Z. Krizanova, V. Smatko, et al., Thin polyaniline and polyaniline/carbon nanocomposite films for gas sensing, *Thin Solid Films*, 519(2011) 4123-7.
- [79] R. Anwane, S. Kondawar, Electrospun Poly(methyl Methacrylate)/Polyaniline Blend Nanofibres with Enhanced Toxic Gas Sensing at Room Temperature, *J. Phys. Sci.* 29(2018) 101-19.
- [80] C. Li, N. Chartuprayoon, W. Bosze, K. Low, K.H. Lee, J. Nam, et al., Electrospun Polyaniline/Poly(ethylene oxide) Composite Nanofibers Based Gas Sensor, *Electroanalysis*, 26(2014) 711-22.

Figures captions:

Scheme 1: Preparation details showing the specific synthesis protocol leading to the formation of PANI composites.

Fig. 1: FTIR spectra of composite PANI/PMMA/PS/MWCNTs (MWCNTs 3.5 wt%), PMMA, PS, and PANI.

Fig. 2: SEM images of a) pure PANI, b) composite (MWCNTs 3.5 wt%) prepared by protocol 2, c) composite (MWCNTs 3.5 wt%) prepared by protocol 1, and d) a zoom on the composite prepared by protocol 1.

Fig. 3: I-V characteristics of composite (PANI/PMMA/PS/MWCNTs) with different MWCNTs contents 0.7 wt% (green), 3.5 wt% (black), 7 wt% (blue) and 10 wt% (red) at room temperature (~28°C).

Fig. 4: Temperature dependence of the resistance for both PANI and PANI composites.

Fig. 5: Sensor response recorded at room temperature (~28°C) and RH of 4%: for (a) PANI/MWCNTs, (b) PANI/PS, (c) PANI/PMMA/PS and (d) PANI/PMMA/PS/MWCNTs towards ammonia gas (50-600 ppm).

Fig. 9: Calibration curves for PANI/PS, PANI/PMMA/PS and PANI/PMMA/PS/MWCNTs as function of NH₃ concentration, measured at room temperature (~28°C) and RH of 4%.

Fig. 7: Sensors responses to 300 ppm of NH₃ exposure at various relative humidity percentage for PANI composites and PANI measured at room temperature (~28°C).

Fig. 10: Sensor response to four sequences of exposure of NH₃ in the lower concentration range (5 - 20 ppm) for the PANI/PMMA/PS/MWCNTs composite, measured at room temperature (~28°C) and RH of 4.5%.

Fig. 9: Selectivity histogram of composite film sensor (PANI/PMMA/PS/MWCNTs) toward different gases at room temperature (~28°C) and RH of 4.5%.

Fig. 10: Sensor response to many cycles of exposure of NH₃ (50 - 600 ppm) for the PANI/PMMA/PS/MWCNTs composite, measured at room temperature (~28°C) and RH of 4.5%.

Table 1: Comparison of the composite sensor performance to other PANI blends-based sensors for NH₃ detection.